Available online at www.sciencedirect.com
ScienceDirect
Journal of Catalysis 246 (2007) 158–165
JOURNAL OF CATALYSIS
www.elsevier.com/locate/jcat

Bimetallic PtSn/C catalysts promoted by ceria: Application in the nonoxidative dehydrogenation of isobutane

J.C. Serrano-Ruiz, A. Sepúlveda-Escribano *, F. Rodríguez-Reinoso

Departamento de Química Inorgánica, Universidad de Alicante, Apartado 99, E-03080 Alicante, Spain

Received 20 October 2006; revised 1 December 2006; accepted 4 December 2006

Available online 4 January 2007

Abstract

A series of bimetallic platinum–tin catalysts supported on CeO_2/C were prepared and tested in the nonoxidative catalytic dehydrogenation of isobutane. Pt–Sn/CeO_2/C catalysts with varying Sn content (Sn/Pt = 0, 0.25, 0.5, and 0.75) were prepared using a co-impregnation method and chlorinated metal precursors. They were characterized by XPS and by CO and ethylene adsorption microcalorimetry at room temperature after in situ reduction treatments. It was found that the presence of cerium in bimetallic catalysts inhibited reduction of tin species, whereas tin facilitated reduction of cerium(IV) to cerium(III). Reduction at 773 K caused a strong decrease in CO saturation coverage for all catalysts studied. For the bimetallic catalysts, a strong interaction between tin and platinum produced significant changes in the initial heat of CO adsorption. The presence of cerium caused a strong decrease in the heat of ethylene adsorption on platinum in catalysts reduced at high temperature. The monometallic Pt catalyst undergoes a fast deactivation with time on stream in the isobutane dehydrogenation reaction. The addition of tin strongly suppresses the deactivation process. It was found that cerium-containing catalysts showed higher isobutene yields compared with their corresponding cerium-free counterparts. The bimetallic catalyst with Sn/Pt = 0.5 showed the best isobutene yield, and it was studied further. This optimized catalyst demonstrated good deactivation behaviour (comparable with the best catalysts reported in the literature). Furthermore, oxidation treatment at a mild temperature (573 K) allowed recovery of nearly all of its catalytic properties.

Keywords: Pt–Sn catalysts; CeO_2; Dehydrogenation; Adsorption microcalorimetry; XPS

1. Introduction

Catalytic dehydrogenation of lower alkanes (propane, isobutane) is of great interest due to the growing demand of propene and isobutene as petrochemical base products. Light alkenes are widely used in industry, because they are involved in such processes as the production of polymers, ethers, nitriles, reformulated gasoline and other materials. The traditional sources of alkenes are both thermal and catalytic hydrocracking used for gasoline production. However, alkene demand is not totally covered by these processes. This has caused a growing interest in the catalytic dehydrogenation of light alkanes, which can be easily obtained from wet natural gas sources [1]. The dehydrogenation of light alkanes to alkenes is a highly endothermic reaction, and conversion is limited by the thermodynamic equilibrium. Thus, the application of high operation temperatures (800–1000 K) is required to obtain an acceptable level of alkane conversion. Under these conditions, undesirable side reactions, such as hydrogenolysis and isomerization, occur with the formation of byproducts and coke deposits, thus producing catalyst deactivation. The coke deposited on the catalyst surface can be removed by oxidation treatments at mild temperatures, allowing the regeneration of catalytic properties.

Platinum catalysts have been widely used in the chemical and petrochemical industries for alkane dehydrogenation. Although a wide variety of catalyst formulations has been reported in the literature, most platinum-based catalysts are characterized by the simultaneous presence of tin. Tin is added in platinum catalysts to alter the product distribution for hydrocarbon conversion through the inhibition of hydrogenolysis, isomerization, and coke formation, and thereby enhance the selectivity and stability in dehydrogenation processes [2–4]. However, if tin is not added to platinum in adequate proportions, decreased

* Corresponding author. Fax: +34 965 90 34 54.
E-mail address: asepul@ua.es (A. Sepúlveda-Escribano).

0021-9517/$ – see front matter
doi:10.1016/j.jcat.2006.12.004

alkane conversion values can result [5,6]. The mechanism by which tin modifies the catalytic behaviour of platinum remains a matter of debate due to the complicated nature of the PtSn systems. Some authors claim that tin modifies the platinum particles by a geometric effect, decreasing the number of contiguous platinum atoms [7,8]. The addition of tin decreases the extent of coke formation and hydrogenolysis reaction, because these undesirable reactions require large ensembles of platinum atoms [9]. In contrast, kinetic results suggest that the dehydrogenation reaction can proceed on small ensembles of surface platinum atoms [10]. A second effect has an electronic nature, by which the presence of tin may change the electronic environment of platinum atoms [11]. It is assumed that coke precursors are not adsorbed on the surface of electronically modified platinum crystals, thus avoiding the deactivation of active sites [12].

On the other hand, it is well known that platinum, when supported on reducible oxides such as CeO_2, can interact with the support after reduction treatments at high temperatures [13]. The onset of this interaction produces a significant change in the chemical properties of the platinum-dispersed phase [14]. Furthermore, it has been determined that the presence of cerium can affect the platinum–tin interaction in the case of bimetallic catalysts [15].

This paper reports a novel type of platinum–tin catalysts, promoted by ceria and supported on activated carbon, which are active and selective for isobutane dehydrogenation. Catalysts were characterized by XPS and adsorption microcalorimetry after different in situ reduction treatments to study the Pt–Sn interaction and evaluate how this interaction is affected by the presence of cerium. A study on deactivation and regeneration of the catalyst with the best performance is also included.

2. Experimental

The CeO_2/C support was prepared by impregnation of the previously degassed carbon (Norit, BET = 790 $m^2\,g^{-1}$) with an acetone solution of $Ce(NO_3)_3{\cdot}6H_2O$ (10 ml of solution per gram of support) at an adequate concentration to obtain a CeO_2 loading of 20 wt%. The impregnated sample was then dried overnight under vacuum at 333 K and calcined in air at 473 K. Pt–Sn/CeO_2/C catalysts were prepared by co-impregnation with acetone solutions containing H_2PtCl_6 (Johnson-Mathey) and $SnCl_2$ (Aldrich, 98%). The excess solvent was removed by flowing nitrogen through the slurry, and the wet solid was dried overnight at 333 K and kept in a desiccator until use. The Sn/Pt atomic ratio was varied from 0 to 0.75, and the nominal platinum content was 2 wt% in all cases. A set of cerium-free Pt–Sn/C catalysts was prepared in the same way to establish the effect of cerium on the properties of the catalysts.

X-ray photoelectron spectra (XPS) were acquired with a VG-Microtech Multilab 3000 spectrometer equipped with a hemispherical electron analyzer and a Mg$K\alpha$ ($h\nu$ = 1253.65 eV, 1 eV = 1.6302×10^{-19} J) 300-W X-ray source. The powder samples were pressed into small Inox cylinders and then mounted on a sample rod placed in a pretreatment chamber and reduced in flowing H_2 for 1 h at 773 K before being transferred to the analysis chamber. Before recording the spectra, the sample was maintained in the analysis chamber until a residual pressure of ca. 5×10^{-7} N m^2 was reached. The spectra were collected at a pass energy of 50 eV. The intensities were estimated by calculating the integral of each peak, after subtraction of the S-shaped background, and by fitting the experimental curve to a combination of Lorentzian (30%) and Gaussian (70%) lines. All binding energies were referenced to the C 1s line at 284.6 eV, which provided binding energy values with an accuracy of ±0.2 eV. The surface Pt/C, Pt/Ce, and Pt/Sn atomic ratios were estimated from the integrated intensities corrected by the atomic sensitivity factors [30].

Differential heats of CO and ethylene adsorption were measured at 300 K in a Setaram BT2.15D heat-flux microcalorimeter as described previously [16]. The microcalorimeter was connected to a high-vacuum (base pressure $<10^{-5}$ Torr) volumetric system using Baratron capacitance manometers for precision pressure measurement (0.5×10^{-4} Torr). The maximum apparent leak rate of the volumetric system (including the calorimetric cells) was 10^{-5} Torr min^{-1} in a system volume of approximately 80 cm^3 (i.e., 10^{-5} μmol min^{-1}). The procedure for microcalorimetric measurements used in this study is described below. Each sample (about 0.25 g) was treated ex situ in ultrapure hydrogen (99.999% with further purification, Air Liquide) for 1 h (4 K min^{-1} ramp, 100 ml min^{-1}) at the desired temperature (473 or 773 K), after which the sample was purged for 1 h at the same temperature in ultra-high-purity helium (99.999% with further purification, Air Liquide) to remove adsorbed hydrogen. Then it was sealed in a Pyrex NMR tube capsule and broken in a special calorimetric cell [16] after the sample had attained thermal equilibrium with the calorimeter. After the capsule was broken, the calorimetric data were collected by sequentially introducing small doses (1–10 μmol) of CO (99.997% with further purification; Air Liquide) or ethylene (99.5%, without further purification) onto the sample until it became saturated. The resulting heat response for each dose was recorded as a function of time and integrated to determine the energy released (mJ). The amount of gas adsorbed (μmol) was determined volumetrically from the dose, equilibrium pressures, and system volume and temperature. The time to pressure equilibration in the microcalorimeter after each dose was approximately 1–15 min, and the heat response was monitored for 20–30 min after each dose to ensure that all heat was detected and to allow the heat response to return to the baseline value. The differential heat (kJ mol^{-1}), defined as the negative of the enthalpy change of adsorption per mole of gas adsorbed, was then calculated for each dose by dividing the heat released by the amount adsorbed.

Reaction kinetic studies of isobutane dehydrogenation were conducted using a stainless-steel apparatus and a glass continuous-flow reactor. Isobutane (99.95%, Air Liquide), hydrogen, and helium as carrier gas were used. A 200-mg catalyst sample was used for each reaction test. All charged catalyst samples were reduced in situ for 1 h in a stream of hydrogen at the same temperature as for the kinetic studies. The reactor inlet and outlet gases were analyzed using a Varian Star 3400 Cx gas

Table 1
XPS Pt $4f_{7/2}$ and Sn $3d_{5/2}$ binding energies for both fresh and reduced at 773 K catalysts

Catalyst	Reduction temperature (K)	Pt $4f_{7/2}$ BE (eV)		Sn $3d_{5/2}$ BE (eV)	
		Un-promoted	CeO_2 promoted	Un-promoted	CeO_2 promoted
Sn/Pt = 0	–	72.4 (100)	72.4 (66) 73.5 (34)	– –	– –
	773	72.1 (100)	71.7 (100)	–	–
Sn/Pt = 0.25	–	72.2 (78) 73.6 (22)	72.6 (62) 74.2 (38)	486.9 (100)	487.0 (68) 488.7 (32)
	773	71.8 (100)	71.7 (100)	485.4 (68) 487.0 (33)	486.2 (100)
Sn/Pt = 0.5	–	71.5 (57) 73.1 (43)	72.5 (69) 73.9 (31)	486.7 (100)	486.9 (68) 488.1 (32)
	773	71.5 (100)	71.8 (100)	485.2 (28) 486.0 (72)	486.5 (100)
Sn/Pt = 0.75	–	71.8 (60) 73.4 (40)	72.4 (61) 74.0 (39)	486.8 (40)	486.8 (49) 487.9 (51)
	773	71.7 (100)	71.7 (100)	485.4 (40) 486.6 (60)	486.3 (100)

chromatograph with a FID detector and a 50 m HP-Al/S column (J&W Scientific) at 313 K.

3. Results and discussion

3.1. X-ray photoelectronic spectroscopy

The Pt $4f_{7/2}$ binding energies in the catalysts both unreduced and after the reduction treatment at 773 K, are reported in Table 1. For the fresh catalysts, and all others except the monometallic unpromoted Pt/C catalysts, two values are given, corresponding to deconvolution of the main peak into two components. The contribution of each peak to the global signal is reported in brackets. The monometallic Pt/C catalyst exhibits a single peak, centred at 72.4 eV, which is shifted to 72.1 eV after reduction at 773 K. The closeness of these two values, considering that platinum is fully reduced to the metallic state after the treatment at 773 K, indicates that some degree of reduction is achieved during impregnation of the carbon support with H_2PtCl_6 and further drying, as reported previously [18]. The Pt $4f_{7/2}$ peak in the fresh bimetallic unpromoted catalysts can be deconvoluted into two contributions. The contribution at lower binding energy can be assigned to metallic platinum and clearly predominates in the catalyst with Sn/Pt = 0.25. The contribution of both signals is closer in the two remaining catalysts (Sn/Pt = 0.5 and 0.75). In any case, the contribution at higher binding energy (73.1–73.6 eV) disappears after reduction at 773 K, with a peak remaining only at 71.5–71.8 eV, which is assigned to metallic platinum. Platinum in the fresh ceria-promoted catalysts shows higher binding energies than in the corresponding ceria-free counterparts. This shift has been observed before [19] and could be a consequence of the interaction with the ceria phase, leading to electronic polarization of the platinum precursor. As in the case of unpromoted catalysts, reduction at 773 K leads to a single peak, centred at about 71.7 eV, demonstrating the presence of metallic platinum [18].

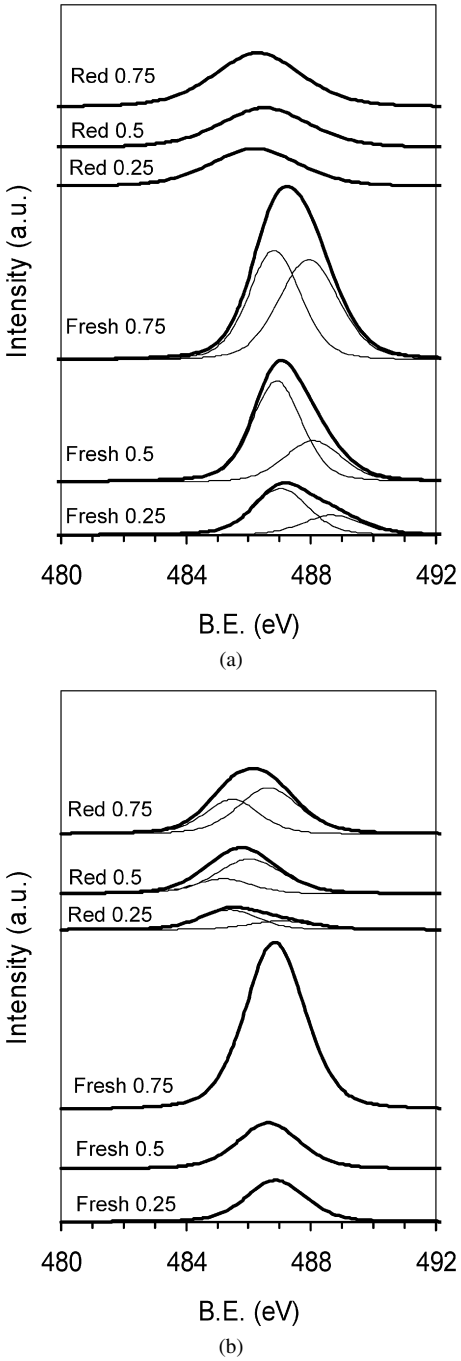

Fig. 1. XPS Sn $3d_{5/2}$ spectra of both fresh and reduced at 773 K bimetallic catalysts. (a) Pt–Sn/CeO_2/C; (b) Pt–Sn/C.

Fig. 1 shows the XPS Sn $3d_{5/2}$ spectra of bimetallic catalysts, both fresh and reduced at 773 K. For the cerium-promoted catalysts (Fig. 1a), the spectra recorded with the fresh samples show 2 peaks at about 487.0 and 488.2 eV (actual values are reported in Table 1). These bands can be assigned to Sn(II) and Sn(IV) chlorinated species, respectively. When the catalysts are reduced, the Sn $3d_{5/2}$ band shifts to lower binding energies, indicating tin reduction. At this point, only one band, centred at about 486.3 eV, can be observed. This peak can be tentatively

Table 2
XPS surface composition for both fresh and reduced at 773 K Pt–Sn/CeO_2/C catalysts

Catalyst	Reduction temp. (K)	Pt/C	Sn/C	Pt/Ce	Sn/Pt	Ce/C	Ce(III) (%)
Pt/CeO_2/C	Unreduced	0.003	–	0.039	–	0.086	32
	773	0.003	–	0.026	–	0.119	38
Sn/Pt = 0.25	Unreduced	0.005	0.014	0.046	2.7	0.104	35
	773	0.004	0.009	0.032	2.2	0.129	41
Sn/Pt = 0.5	Unreduced	0.003	0.018	0.043	5.9	0.079	35
	773	0.004	0.011	0.026	2.6	0.143	45
Sn/Pt = 0.75	Unreduced	0.004	0.033	0.033	8.3	0.112	36
	773	0.004	0.016	0.018	3.9	0.214	50

related to reduced tin as in previous works [18], although the band's position seems to be too high to ensure the presence of metallic tin. It is more likely that a small part of oxidized tin has been reduced to metallic tin, but most remains in an oxidized state even after reduction treatment at 773 K. Furthermore, after the same treatment, cerium-free catalysts showed lower $3d_{5/2}$ binding energies than their corresponding cerium-containing counterparts (Table 1; Fig. 1b). Thus, a new band at about 485.4 eV was observed in cerium-free catalysts after reduction at 773 K, indicative of metallic tin, possibly forming an alloy with platinum. These results indicate that the presence of cerium hinders the reduction of tin species from the metal precursors in these catalysts, as has been reported previously [15]. This may indicate that ceria produces a stabilization effect of oxidized tin species. It is well known that the reduction degree of tin in Pt–Sn bimetallic catalysts depends on a number of factors, the most relevant being the preparation method, the tin precursors, and the support used. In this latter case, the chemical inertness of the support is a very important factor in determining the reduction degree of tin. Thus, if the support used were able to establish a strong interaction with tin (as is the case for ceria, alumina [20], and titania [17]), this would hinder tin reduction. But using a relatively inert support, such as silica [21] or carbon [22], decreases the possibility of a strong tin–support interaction, thus facilitating platinum–tin interaction, possibly facilitating formation of a Pt–Sn alloy phase.

The surface composition of both fresh and reduced catalysts was also studied by XPS (Table 2). The Pt/C atomic ratio remains nearly unchanged (around 0.004) after the reduction treatment in all cases, thus indicating that platinum does not sinter to a significant extent after reduction at high temperature. It is interesting to observe that the Pt/Ce atomic ratio decreases after the reduction treatment in all of the catalysts studied, and this decrease is also accompanied by an increase in the Ce/C atomic ratio. This could indicate a higher amount of surface cerium ions after the reduction treatment. Table 2 also reports the percentages of reduction of Ce for both fresh and reduced (at 773 K) catalysts. These results were obtained from the Ce 3d XPS spectra by a curve-fitting analysis described in detail elsewhere [23]. A certain amount of reduced cerium is present even in the fresh catalysts (around 35%), likely due to photoreduction of Ce(IV) ions during the XPS experiments [24]. The data in Table 2 show that Ce(IV) reduction increases with increasing reduction temperature, and that the reducibility of ceria is higher in bimetallic catalysts. Silvestre-Albero et al. [23], in a study on Pt/CeO_2–SiO_2 and Pt–Zn/CeO_2–SiO_2 catalysts, found a higher amount of surface Ce(III) ions in bimetallic samples. It also can be seen that the amount of reduced cerium increases with tin content, supporting the previous observations.

3.2. Adsorption microcalorimetry

Fig. 2 plots the evolution of the differential heats of CO adsorption versus CO coverage for the Pt–Sn/CeO_2/C catalysts, after in situ reduction at 473 and 773 K. It can be seen that the differential heat of adsorption decreases with increasing coverage, possibly due to adsorption on weaker sites and/or interactions between adsorbed species. At higher coverage, the drastic decrease in the differential heat indicates that surface saturation has been achieved and the physisorption level, taken as 40 kJ mol^{-1}, has been reached. It is interesting to observe that reduction at 773 K produces a significant decrease in CO saturation coverage for Pt/CeO_2/C, from 20 to 6 μmol g^{-1}. This decrease may be the consequence of a strong interaction (induced by the reduction treatment at high temperature) between platinum particles and reduced ceria species (CeO_x) created at the metal–support interface [13]. However, the initial adsorption heat is not affected by this interaction, and its value remains stable after reduction at high temperature (100 kJ mol^{-1}). Conversely, bimetallic catalysts show lower initial heats (except the one with Sn/Pt = 0.75) as well as lower saturation coverages after the reduction treatment at 773 K. Of the ceria-free catalysts (Fig. 3), only the monometallic Pt/C catalyst shows a lower initial heat after reduction at 773 K (107 vs 94 kJ mol^{-1}), whereas no appreciable differences are seen for the bimetallic catalysts (100 kJ mol^{-1}). This indicates that the simultaneous presence of ceria and a second nonactive metal (in this case, tin) in the catalyst formulation produces some improvement in the metal–support interaction after reduction at 773 K [23].

As we noted in our discussion of the XPS findings, metallic tin was not detected in the ceria-containing catalysts after reduction at 773 K (Table 1); therefore, the formation of platinum–tin alloy would not be the cause of the observed decrease in initial heat. More likely, the interaction of platinum particles with oxidized tin species (SnO_x) in their vicinity and, at the same time, a stronger interaction with reduced ceria species due to the presence of tin, could account for the lower initial heat. In the ceria-free bimetallic catalysts, reduction treatment at high temperature caused the reduction to metallic state of a part of oxidized tin species, with possible formation of platinum–tin alloy phase (Table 1). Thus, changes in the initial adsorption heats of CO on platinum in these catalysts would be expected, but this did not occur. However, in the case of Pt–Sn/SiO_2 catalysts, a higher tin content than that used here (Sn/Pt = 2) is needed to produce changes in the initial heats [25].

Fig. 4 plots the differential heat of ethylene adsorption at room temperature versus coverage for catalysts Pt/C and Pt/CeO_2/C previously reduced at 773 K. It can be seen that

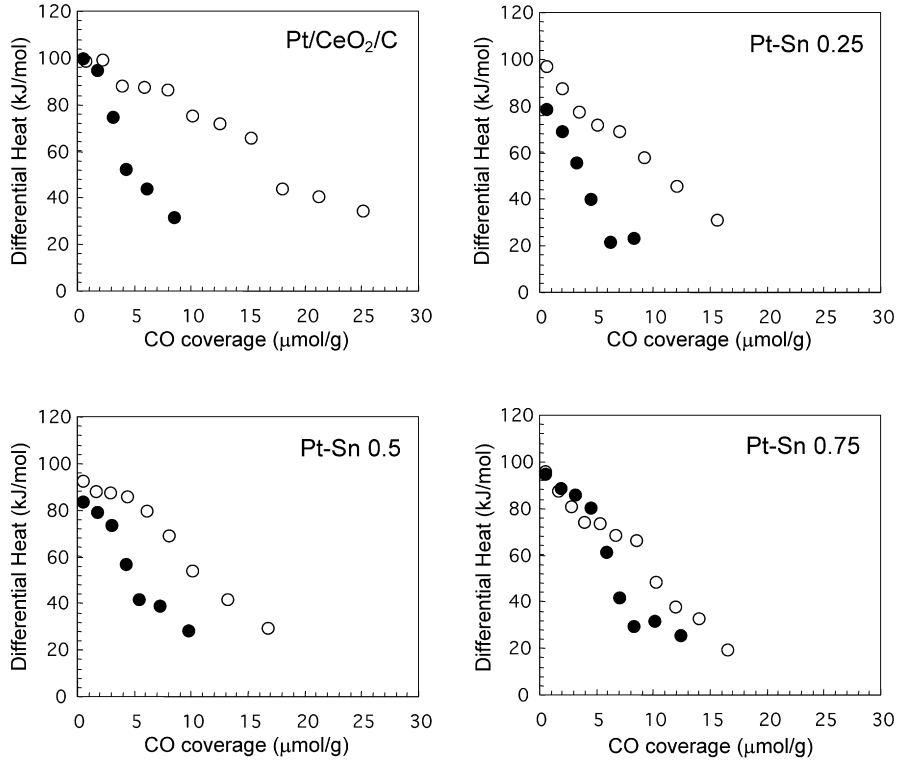

Fig. 2. Differential heats of CO adsorption at 298 K vs CO coverage for Pt–Sn/CeO_2/C catalysts reduced at 473 K (○) or 773 K (●).

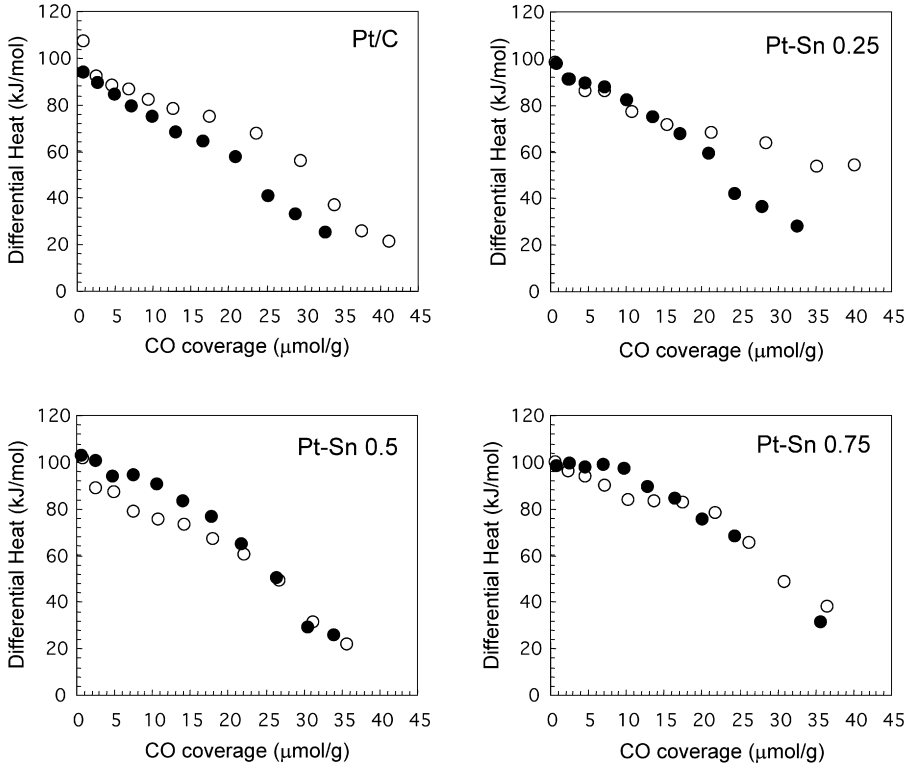

Fig. 3. Differential heats of CO adsorption at 298 K vs CO coverage for Pt–Sn/C catalysts after reduction at 473 K (○) or 773 K (●).

adding ceria to Pt/C leads to a decrease in the heat of ethylene adsorption on platinum. There is a significant decrease in initial heat (from 90 to 65 kJ mol^{-1}) and a slight decrease in the saturation coverage (from 5 to 3 μmol g^{-1}). The plot for the bimetallic Pt–Sn/CeO_2/C catalysts was not included because of the low ethylene saturation coverage, which prevented us from obtaining an accurate measure. These results demonstrates that adding Ce to Pt/C changes the interaction of ethylene with plat-

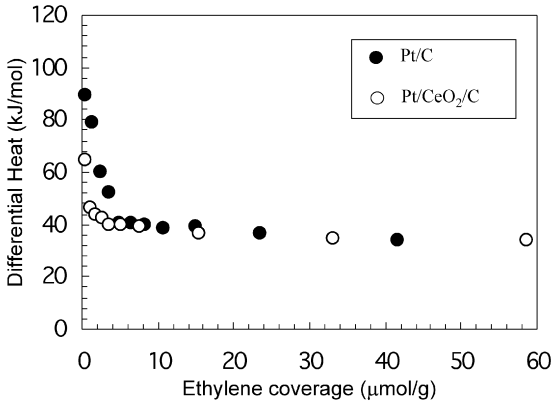

Fig. 4. Differential heats of ethylene adsorption at 298 K after reduction at 773 K.

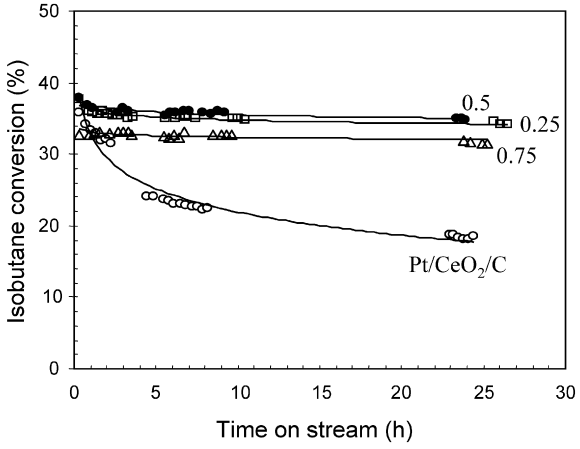

Fig. 5. Isobutane conversions over Pt–Sn/CeO_2/C catalysts at 773 K, 0.016 atm isobutane pressure, 0.098 atm hydrogen pressure, and a WHSV of 4.5 h^{-1}.

inum. As we have seen before, reduction treatment at 773 K leads to Pt/CeO_2/C catalyst to a metal-ceria, producing a significant change in the chemical properties of platinum. This interaction could involve an electronic effect (electrons transfer from reduced ceria, CeO_x, to platinum) and/or a geometric effect (blocking of platinum particles by patches of CeO_x), both of which can lead to a decrease in the strength of ethylene adsorption on platinum.

3.3. Catalytic behaviour

Fig. 5 reports the data for conversion of isobutane versus time on stream for Pt–Sn/CeO_2/C catalysts. These experiments were conducted at 773 K, 0.016 atm isobutane pressure, 0.098 atm hydrogen pressure ($H_2/iC_4 = 6$), and a WHSV of 4.5 h^{-1}. The monometallic Pt/C catalyst underwent a fast deactivation with time on stream (from 36 to 18% conversion in 24 h). When tin was added, deactivation was strongly suppressed. In the case of 0.25 and 0.5 Pt–Sn catalysts, initial conversion increased with regard to the monometallic sample (38% vs 36%). However, adding more Sn (Sn/Pt = 0.75) had a negative effect on conversion (33%). Table 3 shows the percentage of deactivation after 24 h on stream, as well as initial isobutene yields for the catalysts studied. Note that the stability of catalysts increased with tin content, although, in terms of isobutene yield, the Pt–Sn 0.5 catalyst showed the best results. Furthermore, the promotional effect of ceria can be clearly appreciated, because ceria-containing catalysts showed higher isobutene yields than their corresponding ceria-free counterparts. As has been pointed out before, tin seems to be almost completely in an oxidized state in Pt–Sn/CeO_2/C after reduction at 773 K. The distribution of tin species in these catalysts after reduction at 773 K could be as follows: a very small amount of tin would be alloyed with platinum, the rest would be in an oxidized state; some could be isolated from the platinum particles (in strong interaction with the support) and the rest would be in the vicinity of the platinum particles (at the platinum–support interface).

This ionic tin at the platinum–support interface may have two beneficial roles. First, it can decrease the number of contiguous accessible Pt atoms (by a decoration effect), thus inhibiting coke formation and hydrogenolysis. Keep in mind that

Table 3
Percentage of deactivation after 24 h on stream and isobutene yield for Pt–Sn/CeO_2/C catalysts

Catalyst	Deactivation (%)	Isobutene yield (%)	
		Unpromoted	CeO_2 promoted
Pt/CeO_2/C	48.2	23.5	28.3
Sn/Pt = 0.25	9.5	27.0	31.1
Sn/Pt = 0.5	8.2	26.0	33.0
Sn/Pt = 0.75	4.2	27.9	30.4

these undesired reactions require large ensembles of platinum atoms [9], whereas the desired dehydrogenation reaction can proceed on small ensembles of surface platinum atoms [10]. Thus, as a consequence of the reduction of the size of platinum ensembles by ionic tin, no space is available for the build-up of carbonaceous deposits, and, consequently, stability is clearly improved after the addition of tin (Fig. 5). Second, ionic tin can favour the migration of highly dehydrogenated species (coke precursors) from the platinum active site to the support [8].

The presence of ceria also produces two positive effects in this reaction. On one hand, the reduction treatment induces a strong interaction between Pt clusters and particles of reduced ceria (CeO_x). This interaction can lead to decreased adsorption strength of alkenes on platinum (Fig. 4), thereby hindering the successive reaction of these species on the catalyst surface, with the subsequent formation of coke deposits and deactivation of active sites. On the other hand, cerium hinders the reduction of tin in these catalysts (Table 1); therefore, the amount of PtSn alloy is relatively low. It has been proposed that PtSn alloy, although important inhibiting hydrogenolysis and coke formation reactions, is inactive in the dehydrogenation process [3]. Thus, the proportion of PtSn alloy must be kept relatively low with respect to nonalloyed platinum so as to not affect the activity. This could explain the higher conversion values obtained for the ceria-containing bimetallic catalysts in contrast to their ceria-free counterparts. In agreement with these results, Siri et al. [8] observed that in Pt–Sn catalysts supported on SiO_2 and Al_2O_3, the reaction rate for isobutane dehydrogenation decreases with the content of alloyed tin.

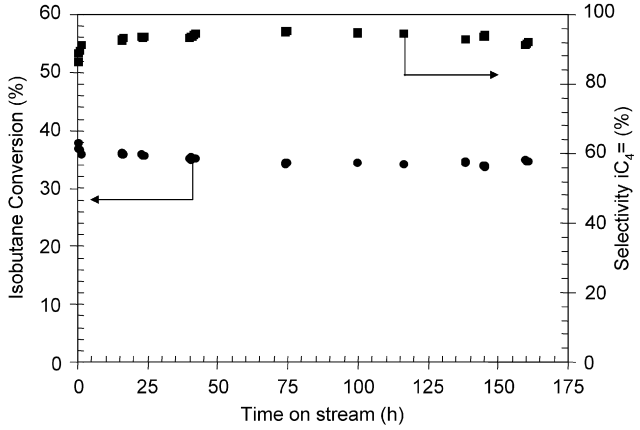

Fig. 6. Isobutane conversions (●) and dehydrogenation selectivities (■) over Pt–Sn(0.5)/CeO_2/C catalyst for long time experiment at 773 K, 0.016 atm isobutane pressure, 0.098 atm hydrogen pressure, and a WHSV of 4.5 h^{-1}.

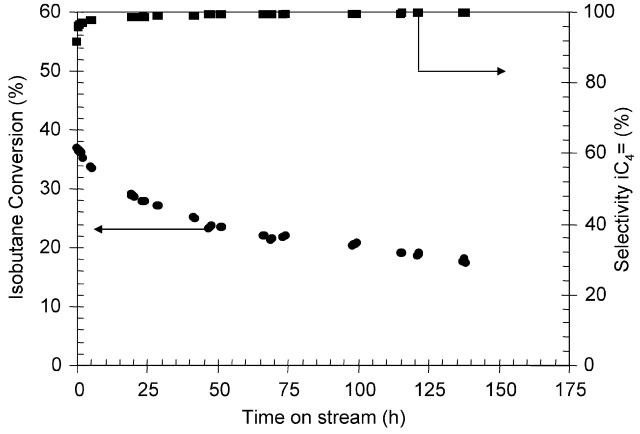

Fig. 7. Isobutane conversions (●) and dehydrogenation selectivities (■) over Pt–Sn(0.5)/CeO_2/C catalyst for long time experiment at 793 K, 0.33 atm isobutane pressure, 0.07 atm hydrogen pressure, and a WHSV of 24.8 h^{-1}.

One of the most important requirements for these catalysts is their stability and regenerability. Considering the catalytic properties as a whole, the Pt–Sn (0.5)/CeO_2/C catalyst is the best system among those studied here. Thus, this optimized catalyst was chosen for further catalytic studies. To test this catalyst's stability, it was submitted to a long-term experiment (175 h) at the same conditions used before (773 K, $H_2/iC_4 = 6$; Fig. 6). After a slight deactivation during the first few hours on stream, conversion remained nearly unchanged until the end of the reaction test. Selectivity to isobutene also remained stable at 95% after an initial period of several hours.

To verify the stability of the optimized catalyst under more severe conditions, a longer catalytic test was carried out at higher temperature and a lower H_2/iC_4 ratio in the feed (793 K, $H_2/iC_4 = 0.2$) with a WHSV of 24.8 h^{-1}. The results for this experiment are plotted in Fig. 7. Under these drastic conditions, conversion decreased with time on stream and was accompanied by a continuous increase in selectivity. The deposition of carbon was responsible for the deactivation. These deposits play the role of inactive species that inhibit undesired reactions, thus explaining the increase in selectivity with time on stream [26].

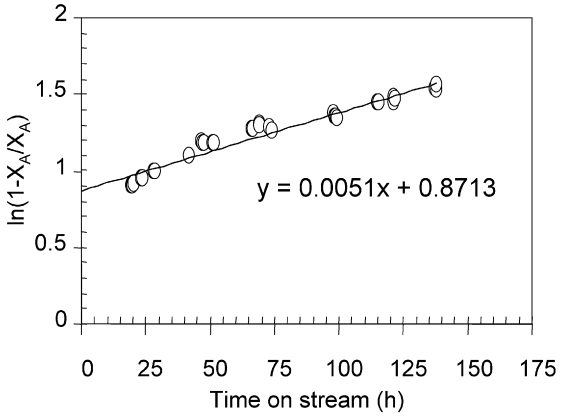

Fig. 8. First order deactivation model fitting of conversion values over Pt–Sn (0.5)/CeO_2/C catalyst for long time experiment at 793 K, 0.33 atm isobutane pressure, 0.07 atm hydrogen pressure, and a WHSV of 24.8 h^{-1}.

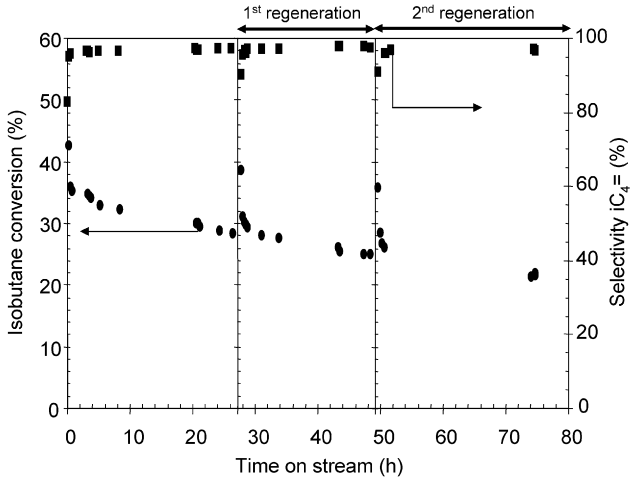

Fig. 9. Isobutane conversions (●) and dehydrogenation selectivities (■) over Pt–Sn(0.5)/CeO_2/C catalyst at 793 K, 0.33 atm isobutane pressure, 0.07 atm hydrogen pressure, and a WHSV of 12.6 h^{-1} after two reaction-regeneration cycles.

To quantify deactivation of the catalyst, an overall first-order deactivation mechanism was assumed. Thus, conversion data were fitted to this first-order deactivation model, allowing us to obtain the deactivation constant (K_d) [27,28],

$$\ln\left[\frac{1-X_A}{X_A}\right] = k_d t + \ln\left[\frac{1-X_{A0}}{X_{A0}}\right]$$

where X_{A0} is the initial conversion of isobutane. The results of this fitting are shown in Fig. 8. Our optimized catalyst has a deactivation constant $K_d = 0.0051$ h^{-1}, comparable to the results obtained by Cortright et al. [7] ($K_d = 0.0078$ h^{-1}) and Waku et al. [29] ($K_d = 0.0041$ h^{-1}), corresponding to the best catalysts reported in isobutane dehydrogenation to date.

To check the regenerability of the Pt–Sn(0.5)/CeO_2/C catalyst, it was submitted to a reaction test for about 25 h under the same drastic conditions as used earlier, but with lower WHSV (12.6 vs 24.8 h^{-1}), to accelerate the deactivation process. After the reaction test, the reactor was cooled to room temperature in a He flow, and treatment in air was carried out at 573 K for 1.5 h. Note that the oxidation treatment at this low tempera-

ture did not produce burning of the carbonaceous support, as verified by a thermogravimetric experiment (not shown). Then, a new dehydrogenation test was carried out (first regeneration) and the process was repeated (second regeneration). The effect of the oxidation treatments on isobutane conversion and selectivity to isobutene is reported in Fig. 9. It can be seen that the oxidation treatments produced recovery of almost all of the initial conversion values, whereas selectivity was not significantly affected. These oxidation treatments at such mild temperatures practically restored the initial dehydrogenation rates (3.1 vs 3.2 $mmol_{isobutene}\ g_{Pt}^{-1}\ s^{-1}$). Furthermore, the percentage of deactivation in 25 h on stream presented only a slight increase with regard to the fresh sample after the regeneration treatment (36% vs 31%). These results indicate that the nature of the active sites is almost recovered after each reaction–regeneration cycle. This fact can be assigned to the close interaction between tin and platinum in this catalyst, in agreement with the XPS and microcalorimetry results given in the previous section.

4. Conclusions

Pt–Sn/CeO_2/C catalysts with different Pt/Sn atomic ratios were prepared by a co-impregnation method and chlorinated metal precursors. From the characterization (XPS and adsorption microcalorimetry) and kinetics results in isobutane dehydrogenation, the following conclusions can be drawn:

1. The preparation method used here allows to both tin and ceria be in close contact with the platinum precursors. Reduction treatment at 773 K affected the catalyst components in different ways: Platinum was completely reduced, cerium was reduced to varying extents (depending on the tin content), and tin remained mainly as ionic tin (due to the presence of cerium).
2. Reduction treatment at 773 K produced a strong interaction between platinum aggregates and partially reduced cerium oxide entities (CeO_x) in their vicinity. This interaction produced a decrease in the amount of CO adsorbed and a weaker interaction of ethylene with platinum. When both promoters are present, the reduction treatment at 773 K caused a decrease in the initial adsorption heat of CO on platinum, thus indicating an improved metal–ceria interaction.
3. These catalysts showed good performance in the dehydrogenation of isobutane at 773 K. The addition of tin is necessary to improve the selectivity and stability of the catalysts by inhibiting undesired reactions. Cerium plays an important role in activity, inhibiting tin reduction and maintaining the amount of alloyed platinum in an adequate level.
4. The catalyst with Sn/Pt = 0.5 showed the best iso-butene yield. This optimized catalyst showed good deactivation behaviour (comparable with that of the best catalysts reported in the literature), whereas oxidation treatments at mild temperatures (573 K) allowed recovery of almost all of its catalytic properties.

Acknowledgments

Financial support was provided by the Comisión Interministerial de Ciencia y Tecnología (projects BQU 2000-0467 and BQU 2003-06150), the Generalidad Valenciana (GRUPOS03-212), and Universidad de Alicante (VIGROB-082). J.C. Serrano-Ruiz thanks Ministerio de Educación y Ciencia (Spain) for an FPI grant. The authors acknowledge the contribution made by Dr. F. Coloma in the XPS measurements.

References

[1] B. Buonomo, D. Sanfilippo, F. Trifiro, in: G. Ertl, H. Knözinger, J. Weitkamp (Eds.), Handbook of Heterogeneous Catalysis, vol. 5, VCH, Weinheim, 1997, p. 2140.
[2] J.M. Hill, R.D. Cortright, J.A. Dumesic, Appl. Catal. A Gen. 168 (1998) 9.
[3] S.M. Stagg, C.A. Querini, W.E. Alvarez, D.E. Resasco, J. Catal. 168 (1997) 75.
[4] O.A. Barias, A. Holmen, E.A. Blekkan, J. Catal. 158 (1996) 1.
[5] M. Ohta, Y. Ikeda, A. Igarashi, Appl. Catal. A Gen. 258 (2004) 153.
[6] S.A. Bocanegra, A. Guerrero-Ruiz, S.R. De Miguel, O.A. Scelza, Appl. Catal. A Gen. 277 (2004) 11.
[7] R.D. Cortright, J.M. Hill, J.A. Dumesic, Catal. Today 55 (2000) 213.
[8] G.J. Siri, J.M. Ramallo-López, M.L. Casella, J.L.G. Fierro, F.G. Requejo, O.A. Ferretti, Appl. Catal. A Gen. 278 (2005) 239.
[9] R.D. Cortright, J.A. Dumesic, J. Catal. 148 (1994) 771.
[10] P. Biloen, F.M. Dautzenberg, W.H.M. Sachtler, J. Catal. 50 (1997) 77.
[11] Z. Paál, A. Gyory, I. Uszkurat, S. Olivier, M. Guérin, C. Kappenstein, J. Catal. 168 (1997) 164.
[12] H. Lieske, A. Sarkany, J. Völter, Appl. Catal. 30 (1987) 69.
[13] S. Bernal, J.J. Calvino, M.A. Cauqui, J.M. Gatica, C. Lopez Cartes, J.A. Perez Omil, J.M. Pintado, Catal. Today 77 (2003) 385.
[14] A. Sepúlveda-Escribano, F. Coloma, F. Rodríguez-Reinoso, J. Catal. 178 (1998) 649.
[15] J.C. Serrano-Ruiz, G.W. Huber, M.A. Sánchez-Castillo, J.A. Dumesic, A. Sepúlveda-Escribano, F. Rodríguez-Reinoso, J. Catal. 241 (2006) 378.
[16] B.E. Spiewak, J.A. Dumesic, Thermochim. Acta 290 (1996) 43.
[17] A. Huidobro, A. Sepúlveda-Escribano, F. Rodríguez-Reinoso, J. Catal. 212 (2002) 94.
[18] F. Coloma, A. Sepúlveda-Escribano, J.L.G. Fierro, F. Rodríguez-Reinoso, Appl. Catal. A Gen. 148 (1996) 63.
[19] M.J. Tiernan, O.E. Finlayson, Appl. Catal. B Environ. 19 (1998) 23.
[20] E. Merlen, P. Becat, J.C. Bertolini, P. Delichère, N. Zanier, B. Didillon, J. Catal. 159 (1996) 178.
[21] J. Llorca, N. Homs, J.L.G. Fierro, J. Sales, P. Ramírez de la Piscina, J. Catal. 166 (1997) 44.
[22] G. Neri, C. Milone, S. Galvagno, A.P.J. Pijpers, J. Schwank, Appl. Catal. A Gen. 227 (2002) 105.
[23] J. Silvestre-Albero, F. Rodríguez-Reinoso, A. Sepúlveda-Escribano, J. Catal. 210 (2002) 127.
[24] M.S.P. Mastelaro, V.R. Nascente, A.O.A. Florentino, J. Phys. Chem. B 105 (2001) 10515.
[25] J. Shen, J.M. Hill, R.M. Watve, B.E. Spiewak, J.A. Dumesic, J. Phys. Chem. B 103 (1999) 3923.
[26] J. Silvestre-Albero, J.C. Serrano-Ruiz, A. Sepúlveda-Escribano, F. Rodríguez-Reinoso, Appl. Catal. A Gen. 292 (2005) 244.
[27] J. Salmones, J.A. Wang, J.A. Galicia, G. Aguilar-Rios, J. Mol. Catal. A Chem. 184 (2002) 203.
[28] O. Levenspiel, Chemical Reaction Engineering, third ed., Wiley, New York, 1999, p. 473.
[29] T. Waku, J.A. Biscardi, E. Iglesia, Chem. Commun. (2003) 1764.
[30] D. Briggs, M.P. Seah, Practical Surface Analysis, vol. 1, second ed., Wiley, New York, 1993.